

Fig. 2 Variation of $C_{n\beta}$ with α .

The results of calculations are presented in Fig. 2. In the calculations, the local angle of attack of chordwise strip RT which is taken in Eq. (3) as $\alpha \sec \Lambda$ was replaced by $(\alpha \sec \Lambda - \alpha_i)$ where α_i is the local induced angle of attack determined from the following relation,

$$C_{Li} = C_{La0} (\alpha \sec \Lambda - \alpha_i) \quad (11)$$

where C_{La0} is the two-dimensional sectional lift curve slope, which for the NACA 0012 ($C_{D01} = 0.006$) wing section equals 0.11 per degree.⁶ Also,

$$C_{Di1} = C_{Da} \cdot \alpha \sec \Lambda = C_{Li} \alpha_i \quad (12)$$

From Fig. 2 we observe that the difference between the present calculation and the experimental data⁵ increases with angle of attack. A possible explanation for this deviation is as follows. In addition to the inherent limitations of the strip theory, the viscous effects ignored in the calculation become predominant at high angles of attack. As the stall propagation for a swept-back wing is from tip to root, the outboard regions which generate significant yawing moment become progressively ineffective as the angle of attack increases. Thus it is obvious that the present calculations compare better with experimental data than Babister's result, which ignores the relative change in dynamic pressure over the wings in side slip. For this wing ($\Lambda = 45^\circ$), the contribution of this dynamic pressure effect to $C_{n\beta}$ is of the same order of magnitude as the other term considered by Babister. Further, it is interesting to note that even zero lift drag makes a contribution to $C_{n\beta}$, indicating that some positive directional stability can be expected from swept-back wings even under cruise condition when lift coefficient is small but the dynamic pressure is large. For higher sweep-back angles, this effect can be much more as shown by Eq. (9) and quite beneficial to the pilot while flying at high lift coefficients under cross wind conditions.

We have shown that the terms not considered by Babister are important and their contribution to wing $C_{n\beta}$ is quite significant. However, the method of computing $C_{n\beta}$ used in the above numerical example can be considerably improved by using more refined approaches such as the vortex lattice method with leading edge or side force suction analogies.

References

- ¹ Babister, A.W., *Aircraft Stability and Control*, Pergamon Press, New York, 1961, pp. 348-358.

² *Engineering Science Data Sheets*, Vol. 3, Aerodynamics, Royal Aeronautical Society, London, 1973, p. A07.01.00.

³ Hoak, D.E., Ellison, D.E., et al., *USAF Stability and Control Datcom*, Air Force Flight Dynamics Laboratory, Flight Division, Wright Patterson Air Force Base, Ohio.

⁴ Roskam, J., "Methods for Estimating Stability and Control Derivatives of Conventional Subsonic Airplanes," University of Kansas, Lawrence, Kansas, 1977, p. 7.5.

⁵ Schlichting, H. and Truckenbrodt, E., *Aerodynamik des Flugzeuges*, Vol. 2, Springer Verlag, Heidelberg, 1969, pp. 70-71, 97.

⁶ Abbott, I.H. and Von Doenhoff, A.E., *Theory of Wing Sections*, McGraw Hill, New York, 1949.

C80-066 Boundary Layer Controls on the Sidewalls of Wind Tunnels for Two-Dimensional Tests

Y. Y. Chan*

National Aeronautical Establishment, Ottawa, Canada

Introduction

IN transonic wind tunnel tests of a two-dimensional airfoil, the growth of the side wall boundary layer and its interaction with the inviscid external flow distorts the spanwise uniformity of the flow across the model and consequently induces errors in the measurements. To lessen the sidewall boundary layer effect, the common practice is to suck off the boundary layer or reduce its thickness ahead of the model. It is hoped that the newly developed boundary layer would be more energetic and therefore cause less trouble in the interaction with the inviscid flow. This method is not very effective and will be discussed further in this Note.

A more effective way to control the growth of the boundary layer is to apply suction at an area of the wall where the model is mounted. The boundary layer at that area is strongly affected by the large pressure gradients induced by the airfoils and the variation of the boundary layer thickness is the greatest. This method is employed in the NAE two-dimensional test facility.¹ In the test section of the tunnel an area of the side walls at which the model is mounted has surfaces made of porous material through which the boundary layer is bled. Because of the large resistance of the porous material, the suction velocity is nearly constant at the whole suction area and is only slightly affected by the pressure variation around the model. The amount of suction can be adjusted until the flow over the portion of the model joining the side wall is parallel to the side wall, and a spanwise uniform two-dimensional condition is established. The optimal condition of suction is determined by observing the flow visualization on the model surface and confirmed by a direct calculation of the boundary layer development on the side wall. In practice, it has been shown that in transonic testing conditions, a nominal suction velocity v_s/u_∞ of 0.005 is adequate for models at maximal lift coefficient. Slight oversuction has no appreciable effects on the flow pattern or the force and pressure measurements. Thus this value is then used for all testing conditions.¹

Received July 10, 1979; revision received Dec. 10, 1979. Copyright © American Institute of Aeronautics and Astronautics, Inc. 1979. All rights reserved.

Index categories: Testing, Flight and Ground; Transonic Flow.

*Senior Research Officer, High Speed Aerodynamics Laboratory. Member AIAA.

This Note presents some results of the side wall boundary layer developments corresponding to the two control methods just described. The detailed examination provides a better understanding of the phenomena with which the merits or the inadequacy of the control methods can be assessed.

Turbulent Boundary Layer Calculations

The side wall boundary layer in a transonic test section is turbulent and compressible in general. In the vicinity of the model the boundary layer is also three-dimensional because of the pressure field induced by the airfoil. The lateral curvature of the streamline, except very close to the leading edge, is small due to the slenderness of the airfoil shape. Thus a small cross-flow formulation can be adopted if the intrinsic streamline coordinates are used for the boundary layer calculations.² If the suction velocity is large as required by the optimal control, the cross-flow is further reduced and in practice only the longitudinal developments of the boundary layer along the streamline coordinates need be considered. The compressible turbulent boundary layer is then calculated by a computer code.³ The details of the analysis and the calculation method can be found in Ref. 4.

Suction Around Model

To demonstrate the boundary layer development on the side wall around the model, calculations have been performed for a typical test case of a transonic airfoil.⁵ The test conditions are as follows:

Airfoil – 16% thick transonic profile

$$M_\infty = 0.599$$

$$\alpha = 3.90 \text{ deg}$$

$$v_s/u_\infty = 0.00555 \text{ (nominal)}$$

$$Re_\infty = 14.54 \times 10^6 / \text{ft}$$

$$C_L = 0.60$$

At the test conditions the flow at the upper surface of the airfoil is supercritical with the local Mach number up to 1.2. The case is chosen for illustration because of its relatively high C_L and a rapid recovery of pressure at the rear portion of the airfoil providing a severe test condition for the suction device. Since the maximum thickness of the airfoil is located near the midchord, the lateral curvature of the profile is still small for most of the airfoil except around the leading edge. Thus the boundary layer computation method discussed in the last section is valid, even for the airfoil with such a thickness.

The suction starts at $x/c = -0.767$ and terminates at $x/c = 0.833$ with respect to the midchord point of 15 in. chord airfoil. The inviscid flowfield around the airfoil is calculated by the transonic small disturbance theory.⁶ The inviscid flow parameters along the streamlines at lateral distances of $y/c = 0.1$ and 0.4 above the airfoil are shown in Fig. 1.

The rapid expansion around the leading edge gives a sharp rise of the pressure gradient parameter $\beta \sim (x/u_e) \cdot (du_e/dx)$ and the gradual recompression downstream induces a negative β , reaching a substantial value near the trailing edge. Away from the airfoil, the pressure decays and the pressure gradient is less severe as shown along the streamline at $y/c = 0.4$. The local suction velocities in terms of the mass flux

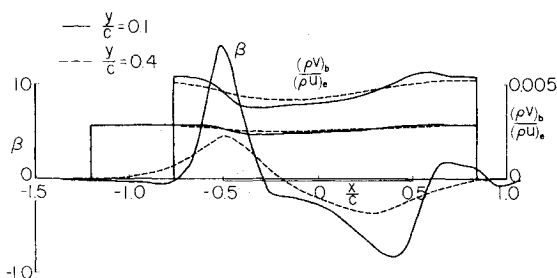


Fig. 1 Distributions of pressure gradient parameter and suction parameter for streamline $y/c = 0.1$ and 0.4 .

ratio $(\rho v)_b / (\rho u)_e$ are also shown. The deviation of the local values from its nominal one is due to the local pressure variations.

For the viscous-inviscid flow interaction up to the first order, the external inviscid flow is affected by the growth of the boundary layer displacement thickness δ^* . The displacement thickness can be considered as an effective body added to the original one or its slope as an additional source distributed on the body surface.⁷ The distributions of δ^* calculated for the conditions shown in Fig. 1 for both without and with suction are shown in Fig. 2.

Without suction, the boundary layer grows gradually against a weak pressure gradient ahead of the airfoil. Near the leading edge, δ^* drops due to the expansion and then grows steadily downstream to a very high value near the trailing edge. This rapid variation of δ^* , especially the bulge formed at the rear portion of the airfoil, induces inflow and outflow from the wall and distorts the spanwise uniformity of the inviscid flow required for the two-dimensional test.

When suction is applied, the boundary layer development changes drastically. Near the airfoil the displacement thickness drops rapidly at the leading edge area due to the double effects of suction and the local acceleration of the flow. Further downstream, the suction inhibits the growth of δ^* even in such severe adverse pressure gradients. The variation of δ^* is more gentle.

For this particular configuration, applying suction exaggerates the reduction of δ^* near the leading edge area. This undesirable effect can be improved by either extending the suction area further upstream or reducing the model size. For a 10 in. chord model, for example, the suction starts at $x/c = -1.15$ and the suction and acceleration effects are well separated. The nominal suction velocity of 0.003 is found to be adequate. This case is also illustrated in Fig. 2. Thus we have demonstrated that, by actively controlling the boundary

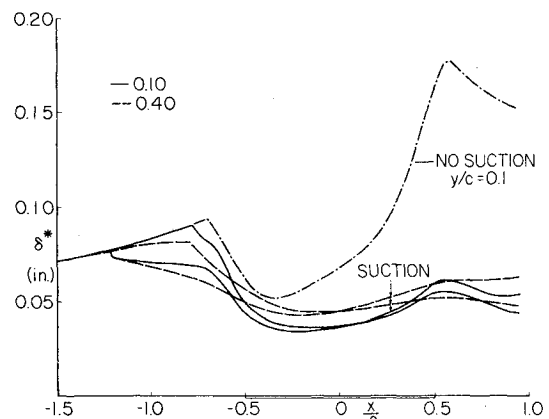


Fig. 2 Variations of displacement thickness δ^* at different conditions.

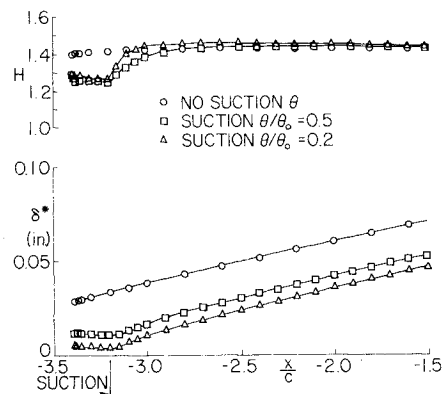


Fig. 3 Recovery of boundary layer after suction.

layer around the airfoil mounting region, the variation of δ^* in the suction region can be reduced to a minimum and the inviscid flow outside the boundary layer is now practically parallel to the sidewall to form a true two-dimensional testing condition.

Suction Ahead of Model

The common method of boundary layer control is to reduce the boundary layer thickness by suction ahead of the airfoil. This method is less effective in controlling the δ^* development as the boundary layer recovers rapidly downstream from the suction area and reverts to the flat plate type. Thus it reacts to the pressure field generated by the airfoil in a similar manner to the case without suction, discussed in the previous section, and large variations of δ^* around the model area result from this. The reduction of initial thickness of the boundary layer appears mainly as a scale effect (Reynolds number effect). The recovery of the boundary layer downstream of the suction region is demonstrated in Fig. 3. The suction area is located at $x/c=2.7$ ahead of the model leading edge.⁸ The growth of δ^* and the variation of form factor H for cases with suction and without suction are shown in the figure. The conditions of the external flow are the same as the case discussed above. The recovery of the suction cases is shown by the rapid increase of form factor H to the value of the flat plate a short distance downstream from the suction boundary, and the δ^* grows at a rate close to that without suction.

The scale effect due to the change of initial boundary layer thickness has been reported by Bernard-Guelle.⁸ He showed that the normal force and the quarter-chord pitching moment decrease as the initial thickness of the boundary layer increases. As shown in Fig. 2, the rapid growth of δ^* at the rear part of the airfoil without suction would undoubtedly induce higher pressure at the upper surface of the airfoil and consequently reduce the normal force and the pitching moment. The pressure induced by the bulging boundary layer can be considered as a small perturbation to the external inviscid flow. Thus the integrated effect of the induced pressure and the boundary layer thickness δ can be correlated linearly. The normal force correlation can then be written as

$$\frac{C_n}{C_{n0}} = 1 - \frac{C}{\sqrt{1-M_\infty^2}} \left(\frac{2\delta}{b} \right)$$

where C_{n0} is the value of C_n with zero δ and b is the width of the test section. The constant C is determined from the data of Ref. 8 and has a value of 1.5, except in the strong interaction region. When the shock on the airfoil is strong, the side wall boundary layer separates after interacting with the shock and the initial thickness has little effect on the flow downstream.

In summary, by applying suction at an area of the sidewall around the model one can actively control the boundary layer growth and consequently the inviscid flow outside the boundary layer can be made practically parallel to the side wall. Without suction, the large variation of the displacement thickness, especially at the rear portion of the airfoil upper surface, causes severe interference to the inviscid flow and distorts the uniformity of the two-dimensional test conditions. Suction applied ahead of the model is much less effective in controlling the boundary layer development, as the boundary layer recovers rapidly after the suction area and responds to the pressure field in a manner similar to that without suction.

References

- Öhman, L.H. and Brown, D., "The NAE High Reynolds Number 15" x 60" Two-Dimensional Test Facility: Description, Operating Experiences and Some Representative Results," AIAA Paper 71-293, Albuquerque, New Mex., March 1971.
- Chan, Y.Y., "Small Cross-Flow in Three-Dimensional Laminar Boundary Layers with Suction or Injection," Aero Report LR-520, National Aeronautical Establishment, Ottawa, Canada, Feb. 1969.

³Chan, Y.Y., "Compressible Turbulent Boundary Layer Computations Based on an Extended Mixing Length Approach," *Canadian Aeronautics and Space Institute Transactions*, Vol. 5, No. 1, March 1972, pp. 21-27.

⁴Chan, Y.Y., Tang, F.C., and Wolfe, S.M., "Analysis of the Boundary Layer Development on the Side Walls of the NAE 2-D Test Facility," Laboratory Technical Report LTR-HA-34, National Aeronautical Establishment, Ottawa, Canada, Nov. 1978.

⁵Eggleston, B., Jones, D.J., and Elfstrom, G.M., "Development of Modern Airfoil Sections for High Subsonic Cruise Speeds," AIAA Paper 79-0687, Williamsburg, Va., March 1979.

⁶Jones, D.J. and Dickinson, R.G., "A Description of the NAE Two-Dimensional Transonic Small Disturbance Computer Method," Laboratory Tech. Rept. LTR-HA-39, National Aeronautical Establishment, Ottawa, Canada, Jan. 1980.

⁷Lighthill, M.J., "On Displacement Thickness," *Journal of Fluid Mechanics*, Vol. 4, 1958, pp. 383-392.

⁸Bernard-Guelle, R., "Influence des Couches Limitées Latérales de Soufflerie dans les Essais Transsoniques en Courant Plan," 12e, Colloque AAAF, Poitiers, 1975.

Experimental Investigation of the Two-Dimensional Asymmetrical Turbulent Wake Behind a Blade

M. A. Ghazi*
King Abdulaziz University, Jeddah, Saudi Arabia

M. I. Rashed†
Cairo University, Cairo, Egypt
and

R. M. El-Taher‡ and K. A. Fathalah§
King Abdulaziz University, Jeddah, Saudi Arabia

Nomenclature

b	= lateral distance between two points of the same actual turbulence intensity
B	= profile width at $T_{e,m} = 0.5$
C	= blade chord
R	= Reynolds number
T_e	= actual turbulence intensity, $T_e = \bar{u}' / \bar{U}$
$T_{e,m}$	= normalized actual turbulence intensity, $T_{e,m} = T_e / T_{e,max}$
$T_{e,max}$	= maximum actual turbulence
U_0	= freestream velocity
\bar{U}	= mean longitudinal velocity
$ \bar{u}' $	= time average of the modulus of longitudinal turbulence component
X	= streamwise distance measured from the blade trailing edge
Y	= lateral distance

Introduction

THE flow in the two-dimensional wake has received wide interest of many investigators in the last few decades. The major part of these studies is experimental, restricted to

Received March 23, 1979; revision received Nov. 19, 1979. Copyright American Institute of Aeronautics and Astronautics, Inc., 1979. All rights reserved.

Index categories: Jets, Wakes, and Viscid-Inviscid Flow Interactions; Aerodynamics.

*Assistant Professor, College of Engineering. Member of AIAA.

†Professor of Aerodynamics.

‡Assistant Professor, College of Engineering, Cairo University.

§Assistant Professor, College of Engineering.